World Journal of

Gastroenterology

World Journal of Gastroenterology

Contents

Contents

ABOUT COVER

Editorial board member of *World Journal of Gastroenterology*, Alfred Gangl, MD, Professor, Department of Medicine 3, Division of Gastroenterology and Hepatology, Medical University of Vienna, Allgemeines Krankenhaus, Vienna A - 1090, Austria

AIMS AND SCOPE

World Journal of Gastroenterology (*World J Gastroenterol*, *WJG*, print ISSN 1007-9327, online ISSN 2219-2840, DOI: 10.3748) is a peer-reviewed open access journal. *WJG* was established on October 1, 1995. It is published weekly on the 7th, 14th, 21st, and 28th each month. The *WJG* Editorial Board consists of 642 experts in gastroenterology and hepatology from 59 countries.

The primary task of *WJG* is to rapidly publish high-quality original articles, reviews, and commentaries in the fields of gastroenterology, hepatology, gastrointestinal endoscopy, gastrointestinal surgery, hepatobiliary surgery, gastrointestinal oncology, gastrointestinal radiation oncology, gastrointestinal imaging, gastrointestinal interventional therapy, gastrointestinal infectious diseases, gastrointestinal pharmacology, gastrointestinal pathophysiology, gastrointestinal pathology, evidence-based medicine in gastroenterology, pancreatology, gastrointestinal laboratory medicine, gastrointestinal molecular biology, gastrointestinal immunology, gastrointestinal microbiology, gastrointestinal genetics, gastrointestinal translational medicine, gastrointestinal diagnostics, and gastrointestinal therapeutics. *WJG* is dedicated to become an influential and prestigious journal in gastroenterology and hepatology, to promote the development of above disciplines, and to improve the diagnostic and therapeutic skill and expertise of clinicians.

INDEXING/ABSTRACTING

World Journal of Gastroenterology (*WJG*) is now indexed in Current Contents®/Clinical Medicine, Science Citation Index Expanded (also known as SciSearch®), Journal Citation Reports®, Index Medicus, MEDLINE, PubMed, PubMed Central and Directory of Open Access Journals. The 2018 edition of Journal Citation Reports® cites the 2017 impact factor for *WJG* as 3.300 (5-year impact factor: 3.387), ranking *WJG* as 35th among 80 journals in gastroenterology and hepatology (quartile in category Q2).

EDITORS FOR THIS ISSUE

Basic Study

Typing of pancreatic cancer-associated fibroblasts identifies different subpopulations

Michael Friberg Bruun Nielsen, Michael Bau Mortensen, Sönke Detlefsen

Michael Friberg Bruun Nielsen, Sönke Detlefsen, Department of Pathology, Odense University Hospital, Department of Clinical Research, University of Southern Denmark, Odense Pancreas Center (OPAC), Odense C 5000, Denmark

Michael Bau Mortensen, Department of Surgery, HPB Section, Odense University Hospital, Department of Clinical Research, University of Southern Denmark, Odense Pancreas Center (OPAC), Odense C 5000, Denmark

ORCID number: Michael Friberg Bruun Nielsen (0000-0003-3244-9438); Michael Bau Mortensen (0000-0002- 7270-5005); Sönke Detlefsen (0000-0002-9466-2333).

Abstract

AIM
To determine whether it is possible to identify different immune phenotypic subpopulations of cancer-associated fibroblasts (CAFs) in pancreatic cancer (PC).

METHODS
We defined four different stromal compartments in surgical specimens with PC: The juxtatumoural, peripheral, lobular and septal stroma. Tissue microarrays were produced containing all pre-defined PC compartments, and the expression of 37 fibroblast (FB) and 8 extracellular matrix (ECM) markers was evaluated by immunohistochemistry, immunofluorescence (IF), double-IF, and/or *in situ* hybridization. The compartment-specific mean labelling score was determined for each marker using a four-tiered scoring system. *DOG1* gene expression was examined by

quantitative reverse transcription PCR (qPCR).

RESULTS
CD10, CD271, cytoglobin, DOG1, miR-21, nestin, and tenascin C exhibited significant differences in expression profiles between the juxtatumoural and peripheral compartments. The expression of CD10, cytoglobin, DOG1, nestin, and miR-21 was moderate/strong in juxtatumoural CAFs (j-CAFs) and barely perceptible/weak in peripheral CAFs (p-CAFs). The upregulation of *DOG1* gene expression in PC compared to normal pancreas was verified by qPCR. Tenascin C expression was strong in the juxtatumoural ECM and barely perceptible/weak in the peripheral ECM. CD271 expression was barely perceptible in j-CAFs but moderate in the other compartments. Galectin-1 was stronger expressed in j-CAFs *vs* septal fibroblasts, PDGF-Rβ, tissue transglutaminase 2, and hyaluronic acid were stronger expressed in lobular fibroblasts *vs* p-CAFs, and plectin-1 was stronger expressed in j-CAFs *vs* l-FBs. The expression of the remaining 33 markers did not differ significantly when related to the quantity of CAFs/FBs or the amount of ECM in the respective compartments.

CONCLUSION
Different immune phenotypic CAF subpopulations can be identified in PC, using markers such as cytoglobin, CD271, and miR-21. Future studies should determine whether CAF subpopulations have different functional properties.

Key words: Pancreatic cancer; Tumour stroma; Cancer-associated fibroblasts; Extracellular matrix; Subtyping; Immunohistochemistry

Core tip: Pancreatic cancer (PC) has a poor prognosis, which may partially be attributed to the abundant desmoplastic stroma, produced by cancer-associated fibroblasts (CAFs). The exact role of CAFs in PC is currently unclear, as these cells exhibited stimulation of cancer cell proliferation *in vitro*, but depletion of these cells promoted cancer progression in animal models. In this study, using immunohistochemistry, immunofluorescence (IF), double-IF, and/or *in situ* hybridization, we identified different immune phenotypic subpopulations of CAFs in PC, which may, at least in part, explain the previously published, partly contradictory data on the role of CAFs in PC. Further studies are needed to elucidate whether certain CAF subpopulations in PC have different functional properties.

INTRODUCTION
Pancreatic cancer (PC) has an extremely poor prognosis with a 5-year survival rate of only 8%[1]. The main reasons for the poor prognosis are probably the late time of diagnosis and the limited response to chemoradiation therapy (CRT)[2,3]. Fibrosis, characterized by excessive extracellular matrix (ECM) production, plays a significant role in PC because invasive cancer cells are accompanied by an intense desmoplastic reaction. The desmoplastic fibrotic stroma can occupy up to 80% of the entire tumour volume[4]. Deposition of ECM in the desmoplastic stroma causes a reduction in tumour elasticity and increases the interstitial pressure, reducing tumour perfusion[5,6].

Cancer-associated fibroblasts (CAFs) are the most important effector cells in the desmoplastic reaction in PC[7]. These cells are mainly generated *via* the activation of quiescent pancreatic stellate cells (qPSCs)[8,9]. CAFs have been suggested to form an "unholy alliance" with cancer cells, each mutually promoting the proliferation of the other[10-12]. CAF-conditioned media has been shown to induce the proliferation and migration of cancer cells[13-15], and vice versa[16]. Additionally, it has been demonstrated that co-injection of CAFs with cancer cells induced tumour growth in mice[14,16]. Studies examining whether CAFs as a whole inhibit or promote tumour growth are conflicting. On the one hand, high stromal activity, *i.e.*, high numbers of α-smooth muscle actin (α-SMA)-positive CAFs, in surgical specimens had a negative prognostic impact in resected PC patients[17-19], and CAFs hampered the effect of CRT and promoted tumour growth and metastasis in cell culture studies[13,20,21]. Furthermore, the combined targeting of CAFs and cancer cells has shown promise as a therapeutic option in *in vitro* studies[22,23]. On the other hand, depletion of the tumour stroma and fibroblast (FB) population promoted tumour growth and reduced survival in genetically engineered mouse models[24,25].

A few recent studies indicate stromal heterogeneity in PC, which, in part, may explain the different conclusions that may be drawn from the abovementioned studies[26-29]. However, further studies regarding the role of CAFs in PC are needed. We therefore aimed to evaluate whether different immune phenotypic subpopulations of CAFs can be identified in PC. We defined four stromal compartments in resection specimens with PC: The juxtatumoural, peripheral, lobular, and septal stroma. The compartment-specific expression of 37 FB and 8 ECM markers was evaluated in tissue microarrays (TMAs) with human PC using immunohistochemistry (IHC), immunofluorescence (IF), double-IF (d-IF) and *in situ* hybridization (ISH).

MATERIALS AND METHODS
Tissue specimens
Tissue specimens for tissue microarrays for IHC, IF, d-IF and ISH analyses: This project was approved by the Ethical Committee of the Region of Southern Denmark (project ID: S-20140168) and the Danish Data Protection Agency (project ID: 15/33101). We ensured that patients had not advocated against the use of their

Table 1 Patient and tumour characteristics

Characteristics		IHC and IF cohort	ISH cohort
Number	*n*	8	21[1]
Age	Mean (yr)	67.0	67.9
	(range)	(46.7-75.9)	(46.7-80.9)
Sex	Female/male	5/3	13/8
Tumour differentiation grade			
Well differentiated (G1)	*n*	0	0
Moderately differentiated (G2)	*n*	8	19
Poorly differentiated (G3)	*n*	0	2
T Stage[2]	T1/T2/T3/T4	0/0/8/0	0/0/20/1
N stage[2]	N0/N1	2/6	5/16
Surgical procedure			
Whipple resection	*n*	5	16
Left-sided pancreatectomy	*n*	3	5

[1]The 21 patient tumours in the *in situ* hybridization cohort also included the 8 tumours from the immunohistochemistry and immunofluorescence cohort;
[2]According to the International Union Against Cancer (UICC) pTNM classification version 7[60]. ISH: *In situ* hybridization; IHC: Immunohistochemistry; IF: Immunofluorescence.

tissue in the Danish registry for the use of tissue in research (Vævsanvendelsesregisteret).

Three TMAs were constructed for the IHC and IF analyses with tissue from eight human pancreatic ductal adenocarcinoma (PDAC) specimens (Table 1). In this study, the term PC is used for PDAC. Normal pancreatic tissue and cores with autoimmune pancreatitis and alcoholic chronic pancreatitis served as controls. Normal pancreatic tissue was obtained from one patient who underwent an operation for a haemangioma in the caudal region of the pancreas, and one patient who underwent a splenectomy. Three additional TMAs were produced for the ISH analyses, resulting in a total of 21 PC tissues (Table 1). The database of the Department of Pathology, Odense University Hospital (OUH), was searched for pancreatic surgical specimens, obtained from January 1, 2016, onwards. Cases that fulfilled the following criteria were included in the study: Specimens were excluded if they contained neuroendocrine neoplasms, cystic tumours, benign lesions or intraductal papillary mucinous neoplasms (IPMNs). Only ductal adenocarcinomas of the pancreas were included after re-evaluation by a pathologist, ensuring that no ampullary or duodenal adenocarcinomas secondarily involving the pancreas were included.

TMAs were constructed from formalin-fixed and paraffin-embedded (FFPE) tissue blocks. Haematoxylin and eosin-stained slides were examined under a microscope, and three 4 mm diameter cores from each PC specimen from appropriate areas were transferred to a virgin block using an automated tissue array machine (TMA Master, 3DHISTECH, Budapest, Hungary). The three tissue cores from each tumour represented the following three different zones: (1) The tumour centre; (2) the invasive front; and (3) the peritumoral pancreatic parenchyma, where inflammation and fibrosis but no cancer cells were present.

Tissue specimens for quantitative reverse transcription PCR analyses: This study was approved by the

Ethical Committee of the Region of Southern Denmark (project ID: S-20150130) and the Danish Data Protection Agency (project ID: 15/51867). All the included tissue samples were stored in the Danish Cancer Biobank. Nine PC specimens (3 females and 6 males with a mean age of 65.2 years) and three normal pancreatic specimens (2 females and 1 male with a mean age of 61.2 years) were obtained from patients who underwent surgery for PC at OUH in the period from January 10, 2014 to January 10, 2015. Benign pancreatic tissue was obtained from representative areas with no trace of malignancy. Gastrointestinal stromal tumour (GIST) tissue served as a positive control. Fresh tissue specimens from surgical resections were transferred directly to a -80 ℃ freezer upon arrival at the Department of Pathology, OUH.

IHC
Four-micrometre sections were cut on a microtome and mounted on FLEX IHC slides (Dako, Glostrup, Denmark). The IHC staining procedures for some antigens were automated, and some were stained manually. Supplementary Table 1 presents details regarding primary antibodies, dilutions, incubation times and epitope retrieval procedures for each antigen.

The automated protocols, including deparaffinization, epitope retrieval and blocking of endogenous peroxidase activity, were performed using either a BenchMark Ultra Immunostainer (Ventana Medical Systems, Tucson, AZ, United States), with the OptiView Detection Kit (Ventana Medical Systems, Tucson, AZ, United States); a Dako Omnis instrument (Agilent, Santa Clara, United States), with the Dako EnVision FLEX visualization system (Agilent, Santa Clara, United States); a Dako Autostainer Link 48 instrument (Agilent, Santa Clara, United States) with PowerVision (Leica Biosystems, Wetzlar, Germany), CSA Ⅱ (Agilent, Santa Clara, United States), and Dako EnVision (Agilent, Santa Clara, United States) detection systems. Heat-induced epitope retrieval (HIER) and non-HIER protocols were tested for antigen retrieval to obtain the highest signal-to-noise ratio. Nuclear counterstaining
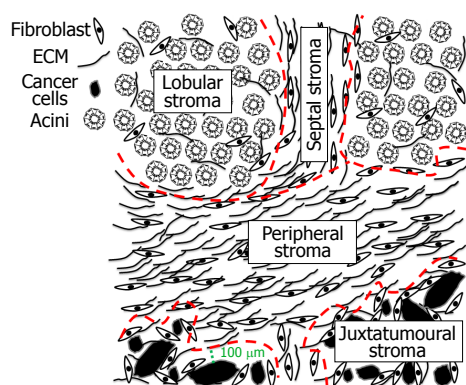
Figure 1 Simplified, schematic depiction of four stromal compartments in surgical specimens with pancreatic cancer. We defined two compartments within the tumour (the juxtatumoural and the peripheral stroma) and two compartments in the surrounding pancreatic parenchyma (the lobular and the septal stroma). The juxtatumoural stromal compartment, containing juxtatumoural cancer-associated fibroblasts and juxtatumoural extracellular matrix, is defined as the stroma at a distance of $\leq$ 100 μm away from the cancer cells. The peripheral stromal compartment, containing peripheral cancer-associated fibroblasts and peripheral extracellular matrix (p-ECM), is located > 100 μm away from the cancer cells. The lobular stromal compartment, containing lobular fibroblasts and lobular ECM, is defined as the stroma located in the intralobular areas, surrounding acinar cells and islets of Langerhans. The septal stromal compartment, containing septal fibroblasts and septal ECM, is defined as the stroma in the perilobular areas, surrounding the pancreatic lobuli. ECM: Extracellular matrix.

was performed with a BenchMark Ultra instrument, using haematoxylin Ⅱ (Ventana Medical Systems, Tucson, AZ, United States), and with the Dako Omnis and Dako Autostainer instruments, using EnVision FLEX haematoxylin (Agilent, Santa Clara, United States). Slides were washed, dehydrated and mounted with coverslips using a Tissue-Tek film coverslipper (Sakura, Alphen aan den Rijn, The Netherlands).

For the manual IHC staining procedures, the tissue sections were dewaxed with xylene and rehydrated with an ethanol gradient in water. A 10-min incubation in 1.5% H_2O_2 (Merck, Darmstadt, Germany) was performed to block endogenous peroxidase activity. Tissue sections were placed in HIER buffers and exposed to three successive steps using a microwave oven (NN-SD450W, Panasonic, Osaka, Japan): (1) 9 min at 900 W; (2) 15 min at 440 W; and (3) 15 min at room temperature (RT). Nonspecific binding was blocked by incubation for 30 min in 2% BSA. The sections were incubated with primary antibody diluted in antibody diluent S2022 (Dako, Glostrup, Denmark) for 60 min at RT or overnight (O/N) at 4 ℃. Unbound primary antibodies were washed away, and the EnVision+ peroxidase/DAB detection system (Dako, Glostrup, Denmark) was used for detection of antigen-bound antibodies. Nuclear counterstaining was performed with Mayers haematoxylin (Fagron Nordic, Copenhagen, Denmark). Slides were washed, dried and mounted with coverslips using Pertex (Histolab, Gothenburg, Sweden).

The following markers were used as IHC and d-IF reference markers for the different stromal cells (Supplementary Table 1): α-SMA (myofibroblasts), CD3 (T

cells), CD20 (B cells), CD68 (macrophages), CD117 (mast cells and stem/progenitor cells), CD163 (macrophages and monocytes), ETS-related gene (ERG, endothelial cells), ionized calcium-binding adapter molecule 1 (IBA-1, macrophages), maspin (adenocarcinoma cells), myeloperoxidase (MPO, neutrophils), synaptophysin (axons and neuroendocrine cells), tryptase (mast cells), and von Willebrand Factor (vWf, endothelial cells).

Definition of four stromal compartments in pancreatic resection specimens with PC: Four different stromal compartments in pancreatic resection specimens with PC were defined: two compartments within the tumour and two in the surrounding pancreatic parenchyma (Figure 1). The stroma inside the tumours was divided into juxtatumoural and peripheral stroma. The juxtatumoural stroma was defined as the stroma located between 0 and 100 μm from the cancer cells (Figure 1)[30]. The peripheral stroma was defined as the stroma located > 100 μm away from the cancer cells. The stroma in the peritumoural pancreatic tissue was divided into lobular and septal stroma. The lobular stroma was defined as the stroma located in intralobular areas, and the septal stroma was defined as the stroma located in perilobular (septal) areas surrounding the pancreatic lobuli (Figure 1).

In each of the four stromal compartments, CAFs and ECM were evaluated separately: Juxtatumoural CAFs (j-CAFs) and juxtatumoral ECM (j-ECM) in the juxtatumoural stroma; peripheral CAFs (p-CAFs) and peripheral ECM (p-ECM) in the peripheral stroma; lobular fibroblasts (l-FBs) and lobular ECM (l-ECM) in the lobular stroma; and septal fibroblasts (s-FBs) and septal ECM (s-ECM) in the septal stroma.

Semiquantitative immunohistochemical scoring: Stained slides were scanned using a 40× objective on a NanoZoomer 2.0HT whole-slide scanner (Hamamatsu Photonics, Hamamatsu, Japan). All quantitative evaluation was performed on digitalized slides using NanoZoomer Digital Pathology (NDP).view2 software (Hamamatsu Photonics).

IHC, ISH and histochemical staining were assessed using a semi-quantitative scoring system on TMAs. The expression of each individual marker was assessed in CAFs/FBs and ECM in the different stromal compartments using a labelling score (LS) from 0 to 4. In this LS scale, 0 indicated no expression, 1 indicated barely perceptible expression, 2 indicated weak expression, 3 indicated moderate expression, and 4 indicated strong expression. Each score was based on the intensity as well as distribution of the expression of the respective markers. The CAF/FB markers were scored in relation to the quantity of activated CAFs/FBs and the ECM markers were scored in relation to the quantity of collagen and reticulin in the respective compartment. α-SMA was used as a reference marker for myofibroblasts (MFBs), and Sirius Red and reticulin were used as reference stains for ECM.

Table 2 Simplified scheme of the expression profiles of 7 of 45 markers that showed a statistically significant difference in expression between the juxtatumoural stroma and peripheral stroma

| | Fibroblast markers | | | | | | | ECM marker |
	α-SMA	CD10	CD271	Cytoglobin	DOG1	miR-21	Nestin	Tenascin C
Juxtatumoural stroma	++++	+++	+	+++	++	+++	++	++++
Peripheral stroma	++++	+	+++	+	-	+	+	+
Lobular stroma	++++	++	+++	+++	+	+	++	++
Septal stroma	++++	+	+++	++	+	+	+	+
Expression in other cells in PC								
Adenocarcinoma cells	-	-	-	-	+	++	-	-
Axons	-	-	-	-	-	-	-	-
Endothelial cells	-	-	-	-	-	-	+++	-
Histiocytes	-	-	-	-	-	-	-	-
Mast cells	-	-	-	-	-	-	-	-
Media myocytes	++++	-	+++	-	-	-	-	-
Neutrophilic granulocytes	-	++	-	-	-	-	-	-
Lymphocytes	-	+++	-	-	-	-	-	-

The expression of these markers in the juxtatumoural, peripheral, lobular and septal stroma is shown, as well as that in adenocarcinoma cells, axons, endothelial cells, histiocytes, mast cells, media myocytes, neutrophilic granulocytes, and lymphocytes. Symbol key: (-) Not expressed in the cell type; (+) barely perceptible expression; (++) weak expression; (+++) moderate expression; (++++) strong expression. α-SMA: α-smooth muscle actin; DOG1: Discovered on gastrointestinal stromal tumours 1; ECM: Extracellular matrix; PC: Pancreatic cancer.

D-IF microscopy

Four-micrometre sections were cut on a microtome and placed on FLEX IHC slides. Tissue sections were dewaxed with xylene and rehydrated with an ethanol gradient in water. HIER protocols were performed for all IF stains. Tissue sections were placed in HIER buffer and exposed to three successive steps using a microwave oven: (1) 9 min at 900 W; (2) 15 min at 440 W; and (3) 15 min at RT. Nonspecific binding was blocked by incubation for 30 min in 2% BSA. The sections were incubated with primary antibody (mouse or rabbit, Supplementary Table 2) diluted in antibody diluent S2022 for 60 min at RT or O/N at 4 ℃. Unbound primary antibodies were washed away, and the specimens were incubated with secondary anti-mouse/rabbit Alexa Fluor-conjugated antibodies (ThermoFisher, Waltham, MA, United States). Unbound secondary antibodies were washed away, and the slides were mounted with DAPI using Vectashield (Vector Laboratories Inc., Burlingame, CA, United States). The following combinations of markers were examined with d-IF: CD10/α-SMA, CD10/ERG, CD10/IBA1, CD271/α-SMA, CD271/ERG, CD271/IBA1, cytoglobin/α-SMA, cytoglobin/CD163, cytoglobin/von Willebrand Factor, DOG1/α-SMA, nestin/α-SMA, and nestin/ERG.

Histochemistry

The sectioning, mounting and deparaffinization steps for the histochemical staining were similar to those for the IHC analyses. The following histochemical stains were used:

Hyaluronic acid: Deparaffinized sections were incubated with 10 μg/mL biotinylated hyaluronic-acid-binding protein (Merck Millipore, Burlington, United States) O/N at 4 ℃. Excess reagent was washed away before incubation with 1:100 HRP-conjugated streptavidin (Dako) for 1 h at RT. DAB substrate (Dako) was applied for detection of hyaluronic-acid-binding protein. Nuclear counterstaining was performed with Mayer's haematoxylin. Slides were washed, dried and mounted with coverslips using Pertex.

Reticulin: This staining was performed by consecutively incubating deparaffinized sections in solutions of 0.5% potassium permanganate (pH 1.5) (3 min, Region Hovedstadens Apotek, Herlev, Denmark), 1% oxalic acid (1 min, Region Hovedstadens Apotek), 2.5% ferric ammonium sulfate (30 s, Region Hovedstadens Apotek), silver solution [30 s, 10% silver nitrate (PanReac AppliChem, Darmstadt, Germany) and 3% sodium hydroxide (Region Hovedstadens Apotek)], 3.6% formaldehyde (30 s, Region Hovedstadens Apotek), and 3% sodium thiosulfate (5 min, Region Hovedstadens Apotek) with intermediate washes in water. Nuclear counterstaining was performed with Mayer's haematoxylin. Slides were washed, dried and mounted with coverslips using Pertex.

Sirius Red: The deparaffinized sections were first stained in Weigert's iron haematoxylin (15 min, Fagron Nordic). Following a washing step, the sections were stained with 0.1% Sirius Red (Ampliqon, Odense, Denmark) in picric acid (15 min, VWR, Søborg, Denmark). The slides were dehydrated and mounted with coverslips using Pertex.

Quantitative reverse transcription PCR

RNA isolation and cDNA preparation: A maximum of 30 mg tissue sample was prepared for RNA isolation from each specimen (nine PC specimens and three normal pancreatic specimens). The tissue was lysed in Buffer RLT (Qiagen, Valencia, California, United States) and homogenized on a T10 Ultra-Turrax disperser (Ika, Staufen, Germany). RNA isolation was performed with the RNeasy Plus Mini Kit (Qiagen) according to the manufacturer's instructions. RNA concentration, purity and integrity were estimated using a NanoDrop

1000 spectrophotometer (Thermo Fisher Scientific, Wilmington, United States) and a BioAnalyzer 2100 (Agilent Technologies, Santa Clara, United States). cDNA synthesis was performed independently on RNA isolated from each specimen according to the manufacturer's instructions from 500 ng of isolated RNA with the High-Capacity cDNA Reverse Transcription Kit (Thermo Fisher Scientific).

Reverse transcriptase quantitative PCR: *Discovered on gastrointestinal stromal tumours 1* (*DOG1*) gene expression was determined by quantitative reverse transcription PCR (qPCR). The PCRs were carried out with the TaqMan gene expression assay (Thermo Fisher Scientific) according to the manufacturer's instructions and run on a QuantStudio 12K Flex real-time PCR system (Thermo Fisher Scientific) using the following PCR conditions: 2 min at 50 ℃, 10 min at 95 ℃ and 50 thermal cycles of 15 s at 95 ℃ and 1 min at 60 ℃. Reactions performed with cDNA from independent specimens were run in triplicate. 18S ribosomal RNA (18S rRNA) and glutaminyl tRNA synthetase (QARS) were used as reference genes for normalization of gene expression because these genes have been previously demonstrated to be the most stable housekeeping genes when comparing normal and PC tissues[31]. Primers and probes were purchased from Thermo Fisher Scientific: Hs00216121_m1 (DOG1), Hs99999901_s1 (18S rRNA) and Hs00192530_m1 (QARS). Relative mRNA expression was calculated using the qBase+ software program (Biogazelle, Gent, Belgium)[32].

ISH
ISH for microRNAs with locked nucleic acid probes: The probe sequences for potential CAF sub-type miR markers (miR-21, miR-199a, miR-214 and miR-221), positive control (miR-126, endothelial marker), and negative control (scramble) are listed in Supplementary Table 3. The listed probes were all double-labelled with digoxigenin (DIG), and ISH was performed on 5-μm thick paraffin sections essentially as described elsewhere[33].The ISH analyses were performed in collaboration with Boye Schnack Nielsen, Bioneer A/S, Hørsholm, Denmark. In brief, the DIG-labelled locked nucleic acid (LNA) probes were detected with alkaline phosphatase-conjugated anti-DIG antibodies followed by incubation with 4-nitro-blue tetrazolium and 5-bromo-4-chloro-30-indolylphosphate (NBT-BCIP) as substrate (Supplementary Table 3). All slides were counterstained with nuclear fast red, dehydrated and mounted using Entellan mounting medium (Fisher Scientific).

COL1A1 mRNA ISH using RNAscope: Detection of COL1A1 mRNA was performed in collaboration with Boye Schnack Nielsen, Bioneer A/S, Hørsholm, Denmark, on the Ventana Discovery platform (Ventana Medical Systems, Tucson, AZ, United States) using RNAscope probes as described elsewhere[34]. Briefly, 5-μm paraffin sections baked (32 min at 37 ℃) and deparaffinized on the instrument, followed by target retrieval (24 min at 97 ℃) and protease treatment (16 min at 37 ℃). Hybridization of probes for 2 h at 43 ℃ was followed by RNAscope amplification (32 min) and detection using the Red (AP) Kit (Roche Diagnostics, Hvidovre, Denmark). The following RNAscope probes (Advanced Cell Diagnostics, Newark, United States) were used: Collagen-I (COL1A1) (cat. No. 401899, target RNA), dihydrodipicolinate reductase, bacterial dapB (cat. No. 312039, negative control), and peptidylprolyl isomerase B (PPIB) (cat. No. 313909, positive control).

Statistical analysis
The mean labelling scores (MLS) for the FB and ECM markers were calculated from the average LS. Column bar graphs were created in GraphPad Prism, ver. 5.01 (GraphPad Software, La Jolla, CA, United States), illustrating the MLS with standard errors of the mean. Ordinal data were compared using the nonparametric Kruskal-Wallis test followed by Dunn's multiple comparison test. A nonparametric test was selected after evaluating the data with the Shapiro-Wilk normality test. Statistical analysis were performed in GraphPad Prism, ver. 5.01. In the graphs, [a]$P < 0.05$, [b]$P < 0.01$, and [c]$P < 0.001$. Statistical analyses of the qPCR data were performed with qBase+ software (Biogazelle, Gent, Belgium). The Mann-Whitney test was used to compare the gene expression of *DOG1* in normal pancreatic tissue with that in PC tissue. The level of statistical significance was set at $P < 0.05$.

RESULTS
Evaluation of FB and ECM markers in PC
A total of 45 markers (32 FB IHC markers, 5 FB ISH markers, 7 ECM IHC markers, and one histochemical ECM stain) were used for semi-quantitative examination with the four-tiered scoring system described above. Most markers were expressed in FBs or ECM. The MLS in the different stromal compartments are shown in Supplementary Table 4. CD10, CD271, cytoglobin, DOG1, miR-21, nestin, and tenascin C exhibited significant differences in expression profiles when comparing j-CAFs/j-ECM with p-CAFs/p-ECM. The expression of these proteins is therefore described in detail below, and the main findings regarding these markers are summarized in Table 2. Regarding the other compartments, galectin-1 ($P < 0.05$) was stronger expressed in j-CAFs *vs* s-FBs, PDGF-Rβ ($P < 0.05$), tissue transglutaminase 2 ($P < 0.05$), and hyaluronic acid ($P < 0.01$) were stronger expressed in l-FBs *vs* p-CAFs, and plectin-1 ($P < 0.05$) was stronger expressed in j-CAFs *vs* l-FBs. The expression of the remaining 33 markers did not differ significantly between compartments. Illustrations regarding the expression of the remaining examined markers in the juxtatumoural and peripheral stroma are presented in Supplementary Figure 1.
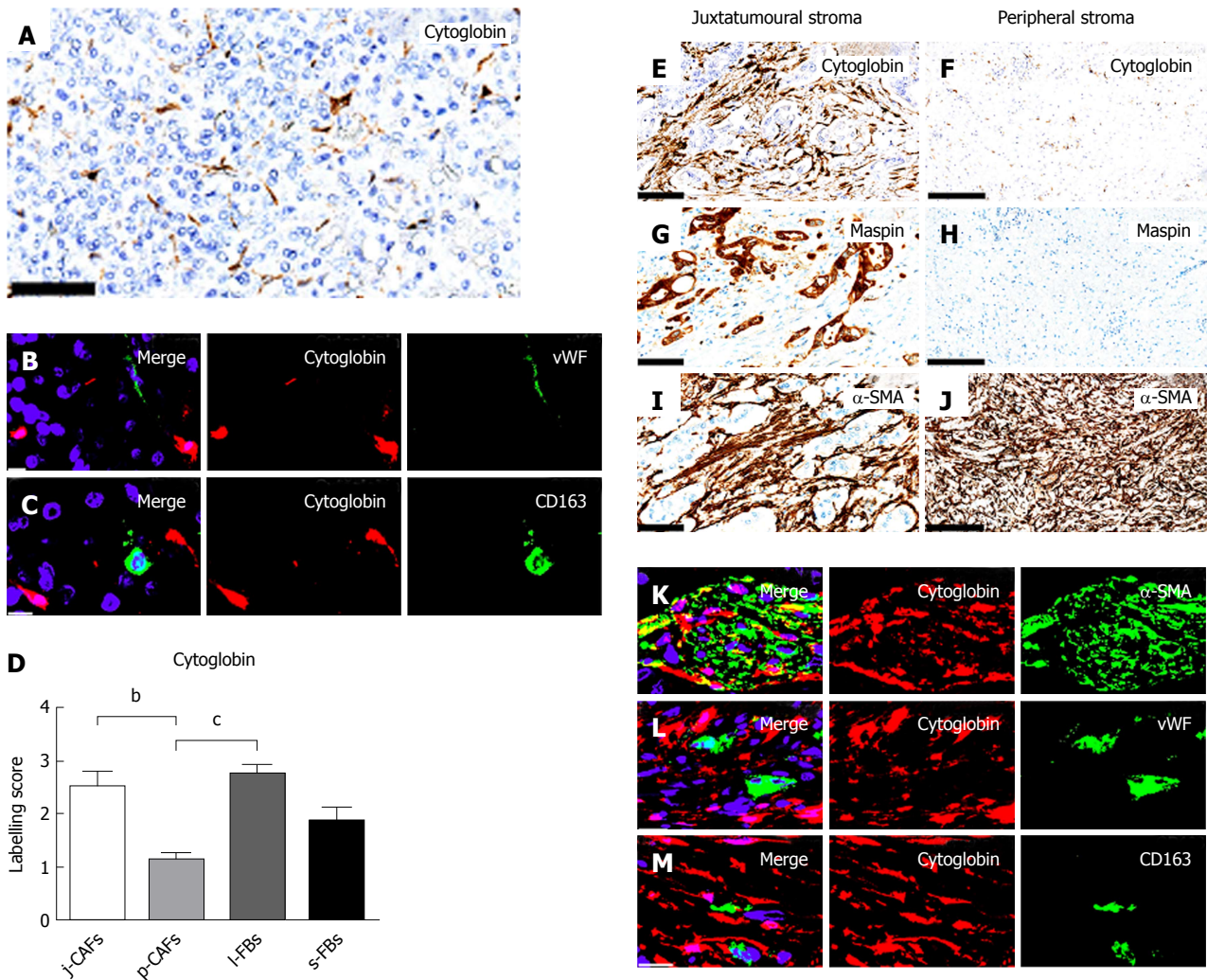
Juxtatumoural stroma   Peripheral stroma

Figure 2 Cytoglobin expression in the normal pancreas and in pancreatic cancer. In the normal pancreas, cytoglobin expression was observed. A: In periacinar quiescent pancreatic stellate cells (cytoglobin immunostaining; scale bars, 50 μm). No co-expression of cytoglobin with; B: The endothelial marker von Willebrand factor (vWf) [double-immunofluorescence (d-IF) of vWF (green) and cytoglobin (red); scale bar, 10 μm]; C: With the histiocyte marker CD163 [d-IF of CD163 (green) and cytoglobin (red); scale bar 10 μm] was observed in the normal pancreas; D: Semi-quantitative mean labelling scores of cytoglobin expression in juxtatumoural cancer-associated fibroblasts (j-CAFs) = 2.5, peripheral cancer-associated fibroblasts (p-CAFs) = 1.1, lobular fibroblasts (l-FBs) = 2.8, and septal fibroblasts = 1.9. Cytoglobin was expressed at significantly higher levels in j-CAFs than in p-CAFs and in l-FBs than in p-CAFs. [b]P < 0.01, [c]P < 0.001; E: Moderate cytoglobin expression in j-CAFs (scale bar, 100 μm); F: In p-CAFs, only barely perceptible cytoglobin expression was observed (scale bar, 250 μm); G: Strong maspin expression in cancer cells surrounded by juxtatumoural stroma (scale bar, 100 μm); H: Peripheral stroma is shown, lacking maspin-positive cancer cells (scale bar, 250 μm). Strong α-smooth muscle actin (α-SMA) expression in I: j-CAFs (scale bar, 100 μm); and J: p-CAFs (scale bar, 250 μm); K: Co-expression of cytoglobin and α-SMA in j-CAFs [d-IF of α-SMA (green) and cytoglobin (red); scale bar, 10 μm]; L: No co-expression of cytoglobin with the endothelial marker vWf in PC [d-IF of vWf (green) and cytoglobin (red); scale bar, 20 μm]; M: No co-expression of cytoglobin with the histiocyte marker CD163 in PC [d-IF of CD163 (green) and cytoglobin (red); scale bar, 20 μm]. j-CAFs: Juxtatumoural cancer-associated fibroblasts; p-CAFs: Peripheral cancer-associated fibroblasts; l-FBs: Lobular fibroblasts; s-FBs: Septal fibroblasts.

Cytoglobin is predominantly expressed in j-CAFs and l-FBs

In normal pancreas, distinct cytoglobin expression was observed in periacinar qPSCs/FBs (Figure 2A). The specificity of cytoglobin for qPSCs/FBs was supported by d-IF analyses with the endothelial marker vWf (Figure 2B) and the histiocytic marker CD163 (Figure 2C), where no co-expression was observed. Semi-quantitative evaluation of the expression of cytoglobin in PC demonstrated significantly higher expression in j-CAFs and l-FBs than in p-CAFs (Figure 2D-J). However, even in j-CAFs, the expression of cytoglobin was lower than that of the myofibroblast marker α-SMA (Figure 2E and I). D-IF analyses demonstrated a co-expression of cytoglobin with α-SMA in stromal fibroblasts in PC (Figure 2K), whereas no co-expression was observed with vWf (Figure 2L) or CD163 (Figure 2M).

CD10 is expressed mainly in j-CAFs

Semi-quantitative evaluation demonstrated significantly higher expression of CD10 in j-CAFs than in p-CAFs and s-FBs in PC (Figure 3A-G). Additionally, CD10 expression was observed in lymphocytes, neutrophils and the epineurium (data not shown). D-IF analyses demonstrated co-expression of CD10 and α-SMA in j-CAFs (Figure 3H), whereas no co-expression was observed with the endothelial marker ERG (Figure 3I) or the macrophage marker IBA-1 (Figure 3J). In normal
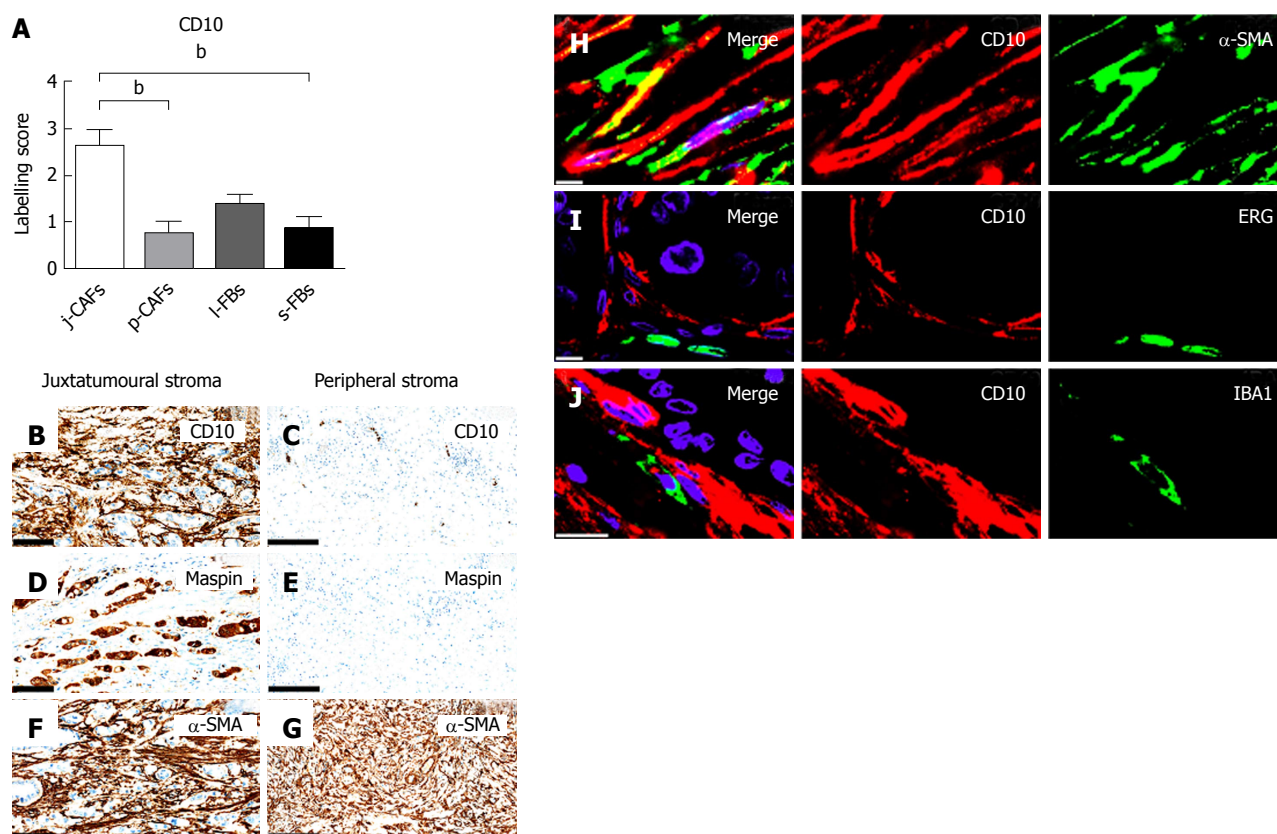
Figure 3 CD10 expression in pancreatic cancer. A: Semi-quantitative mean labelling scores of CD10 in juxtatumoural cancer-associated fibroblasts (j-CAFs) = 2.6, peripheral cancer-associated fibroblasts (p-CAFs) = 0.8, lobular fibroblasts = 1.4, and septal fibroblasts (s-FBs) = 0.9. CD10 is expressed at significantly higher levels in j-CAFs than in p-CAFs and s-FBs. [b]P < 0.01; B: Moderate CD10 expression in j-CAFs (scale bar, 100 μm); C: In p-CAFs, CD10 expression is only barely perceptible (scale bar, 250 μm). Maspin-positive cancer cells are; D: present in juxtatumoural stroma (scale bar, 100 μm) but; E: not in peripheral stroma (scale bar, 250 μm). Strong α-smooth muscle actin (α-SMA) expression in F: j-CAFs (scale bar, 100 μm); and G: p-CAFs (scale bar, 250 μm); H: Co-expression of CD10 and α-SMA in j-CAFs is shown [double-immunofluorescence (d-IF) of α-SMA (green) and CD10 (red); scale bar, 10 μm]. No co-expression of CD10 with; I: the endothelial marker ETS-related gene (ERG) [d-IF of ERG (green) and CD10 (red); scale bar, 10 μm]; or J: with the histiocyte marker IBA1 [d-IF of IBA1 (green) and CD10 (red); scale bar, 20 μm]. j-CAFs: Juxtatumoural cancer-associated fibroblasts; p-CAFs: Peripheral cancer-associated fibroblasts; l-FBs: Lobular fibroblasts; s-FBs: Septal fibroblasts.

pancreas, CD10 expression was observed in lymphocytes, neutrophils, and at the luminal side of the ductal epithelium (data not shown).

CD271 expression is higher in p-CAFs than in j-CAFs

CD271 expression was significantly lower in j-CAFs than in p-CAFs, l-FBs and s-FBs (Figure 4A-G). Additional CD271 expression was observed in large nerves and media myocytes (data now shown). D-IF analyses demonstrated co-expression of CD271 with α-SMA in p-CAFs (Figure 4H) but not with ERG in endothelial cells (Figure 4I) or with IBA-1 in macrophages (Figure 4J). CD271 expression was observed in media myocytes and large nerves of the normal pancreas (data not shown).

Tenascin C expression is higher in j-ECM than in p-ECM

The expression of tenascin C was significantly higher in j-ECM than in p-ECM and s-ECM (Figure 5A-G). Additional tenascin C expression was observed around large peripheral nerves (Figure 5C). In normal pancreas, tenascin C expression was generally low, but some concentrated expression was observed in areas of remodelling and in the tunica media of large blood vessels

(data not shown).

DOG1 is expressed in some j-CAFs but not in p-CAFs

Gene expression of *DOG1* was significantly higher in PC than in normal pancreas (Figure 6A). Semi-quantitative evaluation of DOG1 expression revealed relatively low expression in j-CAFs, which, however, was significantly higher than that in p-CAFs, which were DOG1-negative (Figure 6B-H). Some cancer cells also expressed DOG1 (data not shown). D-IF analyses of DOG1 in combination with α-SMA indicated a co-expression in j-CAFs (Figure 6I). IHC for DOG1 in normal pancreas showed no expression (data not shown).

Nestin expression is higher in j-CAFs and l-FBs than in p-CAFs

Nestin expression was higher in j-CAFs and l-FBs than in p-CAFs (Figure 7A-E). Nestin was also detected in endothelia and in large nerves (data not shown). The expression of nestin was relatively weak and observed in only a fraction of the α-SMA-positive CAFs (Figure 7F). In addition, nestin expression was observed in stromal ERG-positive endothelial cells (Figure 7G). In normal
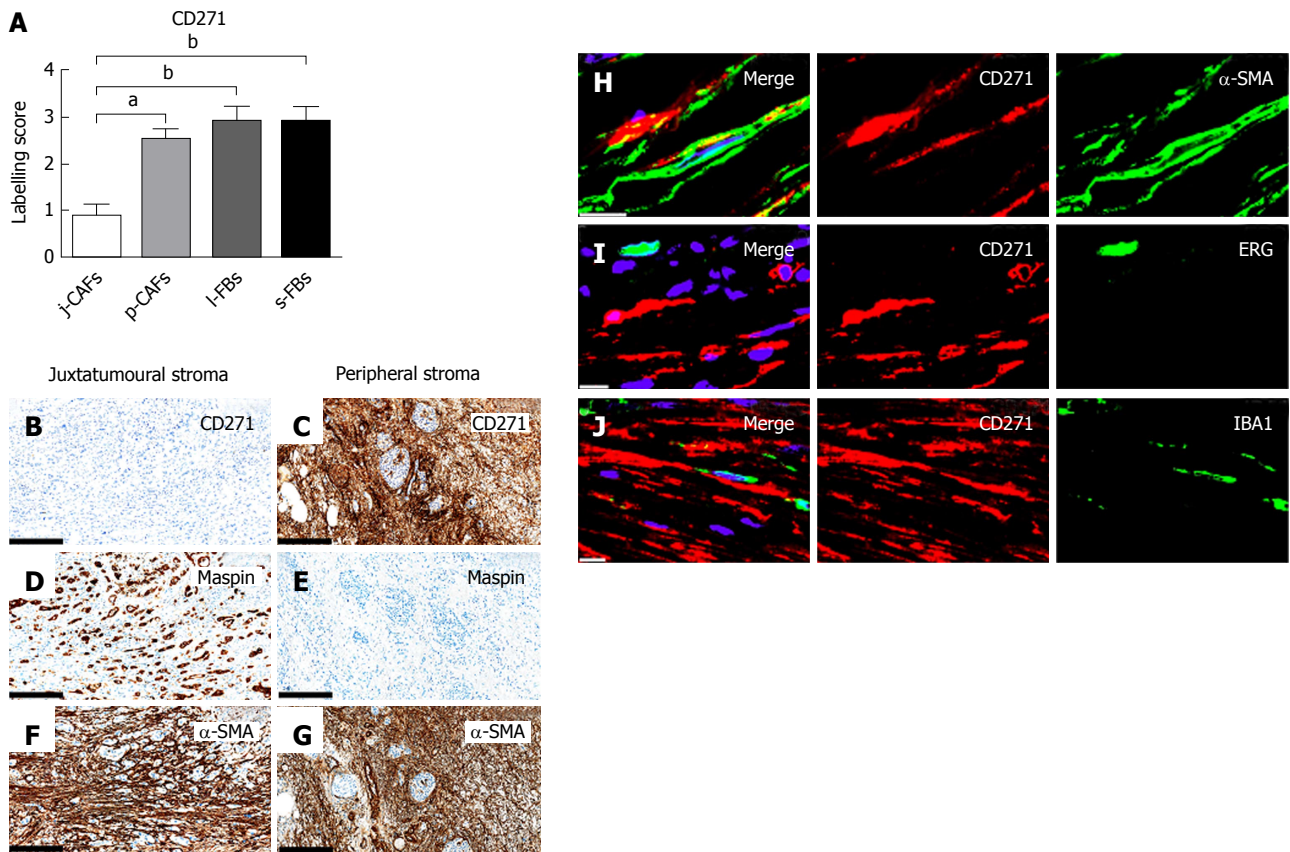
Figure 4 CD271 expression in pancreatic cancer. A: Semi-quantitative mean labelling scores of CD271 in juxtatumoural cancer-associated fibroblasts (j-CAFs) = 0.9, peripheral cancer-associated fibroblasts (p-CAFs) = 2.5, lobular fibroblasts (l-FBs) = 2.9, and septal fibroblasts (s-FBs) = 2.9. CD271 is expressed at significantly higher levels in p-CAFs, l-FBs and s-FBs than in j-CAFs. ${}^{a}P < 0.05$, ${}^{b}P < 0.01$; B: Barely perceptible CD271 expression in spindle-shaped cells in the juxtatumoural stroma; C: In the peripheral stroma, moderate CD271 expression in p-CAFs. Maspin-positive cancer cells are D: present in the juxtatumoural stroma; but E: not in the peripheral stroma. Strong α-smooth muscle actin (α-SMA) expression in F: j-CAFs and G: p-CAFs (scale bars, 250 μm); H: p-CAFs co-express CD271 and α-SMA [double-immunofluorescence (d-IF) of α-SMA (green) and CD271 (red); scale bar 10 μm]; I: No co-expression of CD271 with the endothelial marker ETS-related gene (ERG) [d-IF of ERG (green) and CD271 (red); scale bar, 10 μm]; J: No co-expression of CD10 with IBA1 in histiocytic cells [d-IF of IBA1 (green) and CD10 (red); scale bar, 20 μm]; j-CAFs: Juxtatumoural cancer-associated fibroblasts; p-CAFs: Peripheral cancer-associated fibroblasts; l-FBs: Lobular fibroblasts; s-FBs: Septal fibroblasts.

pancreas, nestin expression was observed exclusively in endothelia and large nerves (data not shown).

miR-21 is expressed mainly in j-CAFs

In PC, miR-21 was expressed at significantly higher levels in j-CAFs than in p-CAFs, l-FBs and s-FBs (Figure 8A-G). Expression of miR-21 was additionally observed in cancer cells (Figure 8B) and large nerves (Figure 8C). Weak miR-21 expression was observed in the ductal epithelia of the normal pancreas (data not shown).

DISCUSSION

In this study, we examined a panel of immunohisto-chemical and miR markers to identify subpopulations of CAFs in PC. We defined four different stromal com-partments in resection specimens of PC, two of which constituted the tumour stroma (the juxtatumoural and peripheral compartments), whereas the other two constituted the stroma of the peritumoural pancreatic parenchyma (the lobular and septal stroma). We found that the expression of cytoglobin, CD10, DOG1, nestin,

and miR-21 was moderate to strong in j-CAFs but only barely perceptible to weak in p-CAFs. The expression of cytoglobin and nestin was additionally significantly higher in l-FBs than in p-CAFs. CD271 exhibited significantly lower expression in j-CAFs than in all other FB/CAF subtypes. Tenascin C was expressed at higher levels in j-ECM than in p-ECM and s-ECM. Hence, our data indicate that the expression pattern cytoglobin^{high}/miR-21^{high}/tenascin C^{high}/CD271^{low} characterizes the juxtatumoural stroma, whereas the opposite pattern is characteristic of the peripheral stroma.

Expression of cytoglobin in qPSCs has been pre-viously demonstrated in mice, rats and humans[35-37]. In the present study, we confirmed cytoglobin as a marker of qPSCs in normal human pancreas and found that it is strongly expressed in j-CAFs. The upregulation of cytoglobin in activated PSCs (aPSCs) has been demonstrated in mice with cerulein-induced pancreatic fibrosis[36,38], but to the best of our knowledge, this is the first report of cytoglobin expression in CAFs in human PC. The expression pattern of nestin was similar to that of cytoglobin, with both markers being expressed at
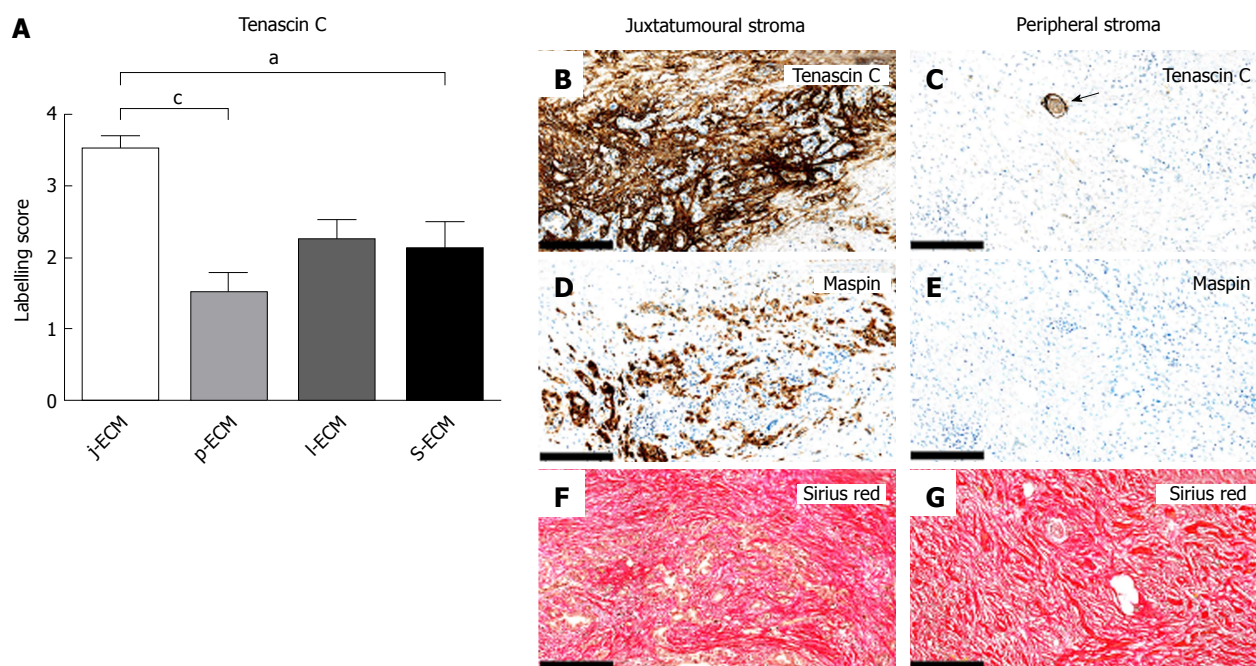
A Tenascin C

B Juxtatumoural stroma — Tenascin C

C Peripheral stroma — Tenascin C

D Maspin

E Maspin

F Sirius red

G Sirius red

Figure 5 Tenascin C expression in pancreatic cancer. A: Semi-quantitative mean labelling scores of tenascin C in juxtatumoural extracellular matrix (j-ECM) = 3.5, peripheral extracellular matrix (p-ECM) = 1.5, lobular extracellular matrix = 2.3, and septal extracellular matrix (s-ECM) = 2.1. Tenascin C is expressed at significantly higher levels in j-ECM than in p-ECM and s-ECM. [a]$P < 0.05$, [c]$P < 0.001$; B: Strong tenascin C expression in the ECM of the juxtatumoural stroma; C: In the peripheral stroma, weak tenascin C expression was observed in the ECM. Tenascin C was abundantly expressed around nerves (arrow). Maspin-positive cancer cells are D: present in the juxtatumoural stroma but; E: not in the peripheral stroma. Strong Sirius Red staining in F: j-ECM and G: p-ECM (scale bars, 250 μm). j-ECM: Juxtatumoural extracellular matrix; p-ECM: Peripheral extracellular matrix; l-ECM: Lobular extracellular matrix; s-ECM: Septal extracellular matrix.

significantly higher levels in j-CAFs and l-FBs than in p-CAFs. Nestin, however, is a less useful CAF marker than cytoglobin because a substantial proportion of nestin expression was observed in endothelial cells. Therefore, nestin has been considered to be a marker for angiogenesis in PC with no prognostic significance[39,40].

Ikenaga *et al*[41] were the first to demonstrate CD10 expression in aPSCs/CAFs isolated from human PC, both *in vitro* and by IHC. They found that only a fraction of aPSCs expressed CD10 and that high expression of CD10 was associated with a poor prognosis[41]. Consistent with our data, the CD10-positive CAFs were predominantly located in the juxtatumoural stroma.

CD271 expression has previously been described in CAFs of human PC, which is consistent with our findings[42]. High stromal CD271 expression was associated with a favourable prognosis, which was consistent with another study that showed that high CD271 mRNA levels were associated with a favourable prognosis[42,43]. Interestingly, CD271-positive CAFs were specifically located "on the edge rather than the centre of the tumours", which is consistent with our data that demonstrated that CD271 expression was significantly higher in all other compartments than in the juxtatumoural compartment[42]. Recently, a diffuse pattern of CD271 expression was reported in PC, predominantly in the "perilesional compartment"[29]. Notably, the perilesional compartment seems to include the juxtatumoural as well as peripheral stroma, indicating that the expression pattern of CD271 was in accord with our data.

The expression of DOG1 in PC has not been fully elucidated, but one study reported the absence of DOG1 expression in a majority of PC cases[44]. By IHC, we observed no DOG-1 expression in normal pancreas but weak expression in cancer cells and in j-CAFs. Upregulation of DOG1 in PC compared to normal pancreas was confirmed by qPCR for DOG1 mRNA. In contrast, it is well known that miR-21 is upregulated in CAFs in different types of human cancer, including breast and PC[45-48], which was also observed in this study. We found that miR-21 was predominantly expressed in j-CAFs compared to other FB/CAF subtypes. miR-21 expression was significantly higher in aPSCs/CAFs than in qPSCs isolated from normal human pancreas, and inhibition of miR-21 with antisense oligonucleotides decreased PSC migration and invasive capacity[49]. Furthermore, high stromal miR-21 levels were associated with a poor prognosis of PC[48]. These findings, taken together with our data, support the view that j-CAFs, in particular, may promote PC growth.

Tenascin C is upregulated in PC and chronic pancreatitis at the mRNA and protein levels[50-52]. Esposito reported that tenascin C was expressed exclusively around neoplastic glands in PC and the expression increased from low-grade precursor lesions to invasive PC[51], which is consistent with our findings. However, the prognostic significance of tenascin C in PC is questionable, as one study showed tenascin C to be prognostic factor in PC[53], whereas another did not[50]. Administration of tenascin C promoted cancer cell growth
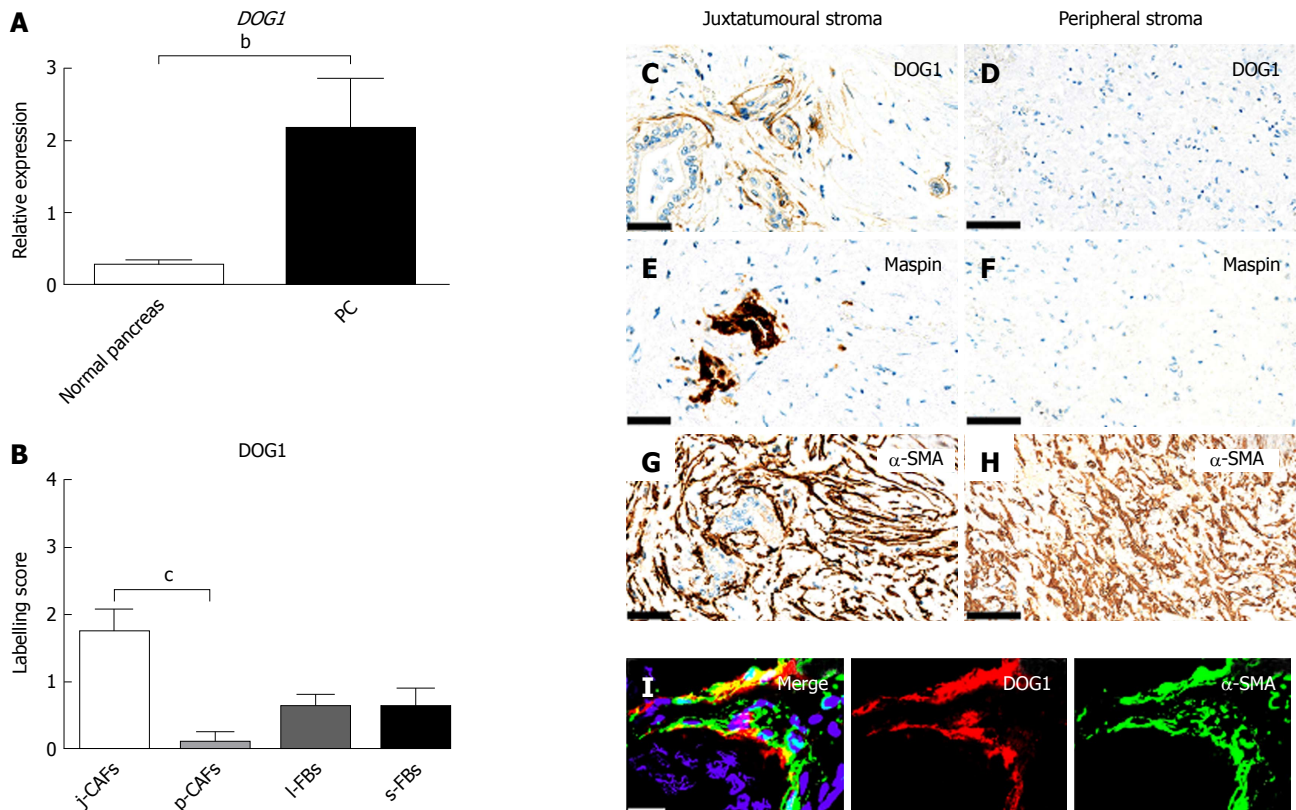
Figure 6 *DOG1* gene and DOG1 protein expression in pancreatic cancer. A: Expression of the *DOG1* gene was significantly upregulated in pancreatic cancer compared to normal pancreatic specimens. [b]$P < 0.01$; B: Semi-quantitative mean labelling scores of DOG1 in juxtatumoural cancer-associated fibroblasts (j-CAFs) = 1.8, peripheral cancer-associated fibroblasts (p-CAFs) = 0.1, lobular fibroblasts = 0.6, and septal fibroblasts = 0.6. DOG1 is expressed at significantly higher levels in j-CAFs than in p-CAFs. [c]$P < 0.001$; C: Weak DOG1 expression in spindle-shaped cells in the juxtatumoural stroma. Some adenocarcinoma cells also expressed DOG1 (scale bar, 50 μm); D: No DOG1 expression was observed in the peripheral stroma (scale bar 100μm). Maspin-positive cancer cells are E: present in the juxtatumoural stroma (scale bar, 50 μm); but F: not in the peripheral stroma (scale bar, 100 μm). Strong α-smooth muscle actin (α-SMA) expression in G: j-CAFs (scale bar, 50 μm); and H: p-CAFs (scale bar, 100 μm); I: j-CAFs co-express DOG1 and α-SMA [double-immunofluorescence of α-SMA (green) and DOG1 (red); scale bar, 20 μm]. j-CAFs: Juxtatumoural cancer-associated fibroblasts; p-CAFs: Peripheral cancer-associated fibroblasts; l-FBs: Lobular fibroblasts; s-FBs: Septal fibroblasts; PC: Pancreatic cancer.

and migration *in vitro*[54], and it could be speculated that a tenascin C-rich stroma is characteristic of a tumour-promoting niche. Hayasaki *et al*[55] divided surgical PC specimens after neoadjuvant therapy (NAT) in high and low NAT responders. Expression of tenascin C was significantly higher in low responders than in high responders, indicating that tenascin C may be a marker of poor response to NAT, supporting the view that j-CAFs and the ECM produced by these cells promote cancer cell growth by being involved in an "unholy alliance" with the cancer cells[55].

Reports on whether CAFs act in a tumour-promoting or tumour-inhibiting manner are conflicting[56]. Our data may partly explain these contradictions, as these data indicate that CAFs do not represent a homogeneous but rather a heterogeneous population. In 2002, Iacobuzio-Donahue *et al*[26] examined the compartmentalized expression of 12 genes in PC using ISH. Three genes (*MMP11*, *Apolipoprotein C-1* and *Apolipoprotein D*) were exclusively expressed in the juxtatumoural stroma[26]. A recent study demonstrated CAF heterogeneity in PC using IF and ISH, which was consistent with our data[27]. CAFs in the juxtatumoural stroma expressed fibroblast

activation protein (FAP) and exhibited elevated levels of α-SMA, whereas the remaining CAFs expressed FAP and exhibited low levels of α-SMA[27]. In mouse models of PC and breast cancer, heterogeneous expression of S100A4, α-SMA, platelet-derived growth factor receptor-beta (PDGF-Rβ) and neuron-glial antigen 2 (NG2) chondroitin sulfate proteoglycan in CAFs was reported, but without description of the precise localization in the tissue[28]. Another recent study defined different pancreatic stromal compartments (periacinar, periductal, inter-/perilobular, and perilesional) and observed stromal heterogeneity in PC and pancreatitis[29]. In particular, α-SMA, tenascin C, osteonectin and NT-3 were highly expressed in the perilesional compartment, which is consistent with the results of the present study.

The use of TMAs in this study allowed us to examine numerous markers in many PC cores simultaneously under the same laboratory conditions. However, important information could potentially have been missed if certain important stromal areas were not included in the TMAs, which is a possible limitation of this study. We addressed this challenge by selecting three tissue cores representing different stromal areas from each
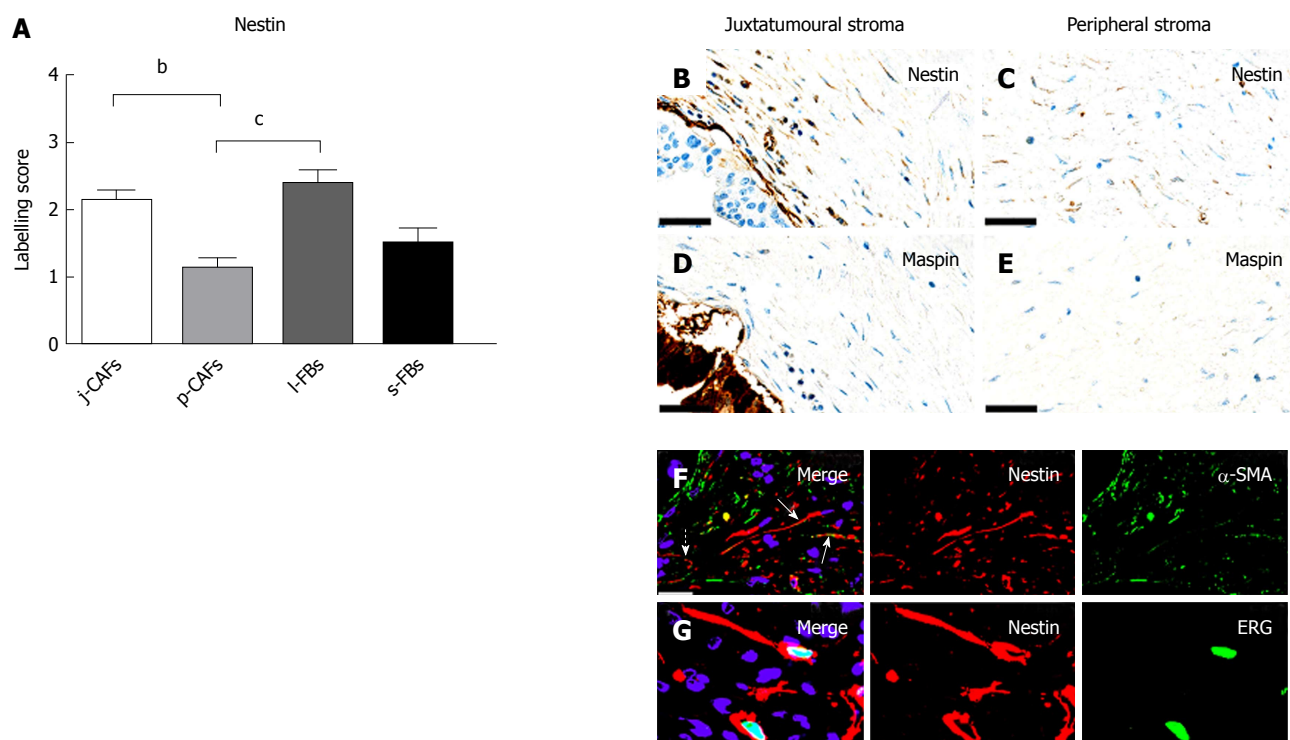
Figure 7 Nestin expression in pancreatic cancer. A: Semi-quantitative mean labelling scores of nestin in juxtatumoural cancer-associated fibroblasts (j-CAFs) = 2.1, peripheral cancer-associated fibroblasts (p-CAFs) = 1.1, lobular fibroblasts (l-FBs) = 2.4, and septal fibroblasts (s-FBs) = 1.5. Nestin is expressed at significantly higher levels in j-CAFs and l-FBs than in p-CAFs. [b]$P < 0.01$, [c]$P < 0.001$; B: Weak nestin expression in a small fraction of spindle-shaped cells in the juxtatumoural stroma; C: Barely perceptible nestin expression in the peripheral stroma. Maspin-positive cancer cells are D: present in the juxtatumoural stroma but; E: not in the peripheral stroma (scale bars, 50 μm); F: Some j-CAFs co-express nestin and α-smooth muscle actin (α-SMA) (closed arrows). Additional expression was observed in α-SMA-negative endothelia (dotted arrow) [double-immunofluorescence (d-IF) of α-SMA (green) and nestin (red); scale bar, 20 μm]; G: Nestin and ETS-related gene (ERG) are co-expressed in endothelial cells [d-IF of ERG (green) and nestin (red); scale bar, 10 μm]. j-CAFs: Juxtatumoural cancer-associated fibroblasts; p-CAFs: Peripheral cancer-associated fibroblasts; l-FBs: Lobular fibroblasts; s-FBs: Septal fibroblasts.

Figure 8 miR-21 expression in pancreatic cancer. A: Semi-quantitative mean labelling scores of miR-21 in juxtatumoural cancer-associated fibroblasts (j-CAFs) = 2.2, peripheral cancer-associated fibroblasts (p-CAFs) = 0.8, lobular fibroblasts (l-FBs) = 1.0, and septal fibroblasts (s-FBs) = 1.1. miR-21 is expressed at significantly higher levels in j-CAFs than in p-CAFs, l-FBs and s-FBs. [b]$P < 0.01$, [c]$P < 0.001$; B: Moderate miR-21 expression in spindle-shaped cells in the juxtatumoural stroma (insert). Adenocarcinoma cells also expressed miR-21; C: Expression of miR-21 in the peripheral stroma was barely perceptible. Large nerves expressed miR-21 (arrow). Maspin-positive cancer cells are D: present in the juxtatumoural stroma; but E: not in the peripheral stroma. Strong α-smooth muscle actin expression in F: j-CAFs; and G: p-CAFs (scale bars, 500 μm). j-CAFs: Juxtatumoural cancer-associated fibroblasts; p-CAFs: Peripheral cancer-associated fibroblasts; l-FBs: Lobular fibroblasts; s-FBs: Septal fibroblasts.
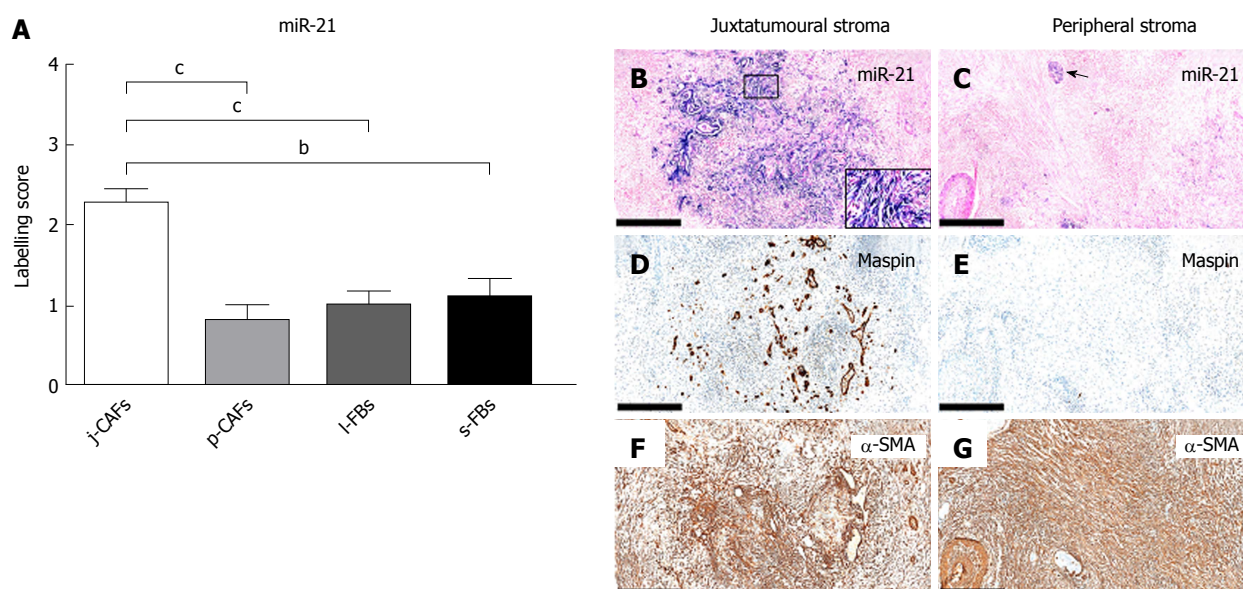
tumour. We defined four different stromal compartments in resection specimens of PC. It could be argued that such a strategy is somewhat simplistic. However, this strategy provided a framework, enabling us to score the expression of the biomarkers in these stromal compartments. It may also be argued that the cut-off distance of 100 μm from the tumour cells to distinguish the juxtatumoural from the peripheral stroma was arbitrary. However, the same definition was previously applied in other studies of the PC stroma, enabling direct comparison between our data and those of these previous studies[30].

Several studies have demonstrated that the stroma plays an important role in PC progression and influences the effect of conventional CRT[6,13,21,57]. Hence, modulation of the stroma, particularly of CAFs responsible for ECM synthesis, may hold promise for new treatment strategies for PC[57-59]. Thus far, these efforts have proven unsuccessful. Based on data from the present study, it is tempting to speculate that j-CAFs, located in close vicinity to cancer cells and characterized by strong expression of markers such as CD10, cytoglobin, DOG-1, and miR-21, may promote the proliferation and invasion of cancer cells, whereas p-CAFs, located at a greater distance from the cancer cells than j-CAFs and strongly expressing CD271, may inhibit the growth of cancer cells. This view is supported by published data that indicate a negative prognostic value for some of our j-CAF markers, namely, CD10 and miR-21[41,48], whereas CD271, a p-CAF marker, held positive prognostic value for PC[42,43]. To our knowledge, this is the first report of cytoglobin expression in human PC, and future studies should examine whether this marker holds prognostic value for PC. Future studies should also examine whether j-CAFs and p-CAFs differ in their effects on cancer cell growth *in vitro*. Finally, it is tempting to speculate that future therapies may aim to specifically modulate the CAF activity by targeting j-CAFs and p-CAFs selectively.

In conclusion, our data show that different immune phenotypic subpopulations of CAFs can be identified in PC by using a panel of markers such as cytoglobin, CD271, and miR-21. Further studies are needed to elucidate whether certain CAF subpopulations in PC hold prognostic value or have different functional properties.

ARTICLE HIGHLIGHTS

Research background
The prognosis of pancreatic cancer (PC) patients remains extremely poor, and unlike other major forms of cancer, there has been no significant improvement in survival rates in recent years. This poor prognosis is mainly due to late-stage diagnosis and limited response to treatment. Hence, continued research into this devastating disease is urgently needed.

PC is characterized by abundant desmoplasia in the stroma surrounding the cancer cells. The desmoplastic stroma consists predominantly of the extracellular matrix (ECM) produced by cancer-associated fibroblasts (CAFs). The exact role of the desmoplastic stroma in PC progression remains unclear. Some studies have indicated that high stromal activity had a negative prognostic impact in resected PC patients, whereas stromal depletion of the entire fibroblast (FB) population promoted tumour growth in genetically

engineered mouse models. We hypothesize that these conflicting studies could be explained by CAF heterogeneity in the desmoplastic stroma of PC, with some CAFs promoting and other CAFs hampering tumour growth.

Research motivation
CAFs are the main effector cells in the desmoplastic reaction in PC. However, it is currently unclear whether CAFs are promoters or inhibitors of tumour growth. Extensive effort has been made to design therapies that target the stromal compartments, including CAFs, in PC, but to date, these efforts have had limited success. This limited success is highlighted by a continually high mortality rate among PC patients. Identification of a panel of markers that could distinguish CAF subtypes would allow researchers to perform subsequent studies to determine the prognostic significance and precise functional properties of these subtypes in PC. Further, it could be speculated that future targeted therapies should be designed to specifically modulate the activity of certain CAF subtypes in PC.

Research objectives
The present study aimed to determine whether it is possible to identify markers that can distinguish different immune phenotypic subpopulations of CAFs in PC. After examining 45 CAF and ECM markers, we found that CD10, CD271, cytoglobin, DOG1, miR-21, nestin, and tenascin C are significantly differentially expressed in the juxtatumoural stroma versus the peripheral stroma in PC. Furthermore, a panel of the markers cytoglobin, CD271, and miR-21 allows the distinction of juxtatumoural and peripheral CAFs (j-CAFs and p-CAFs) in PC. Future studies should examine whether j-CAFs and p-CAFs hold prognostic value and/or have different functional properties in PC.

Research methods
The present study was predominantly based on immunohistochemistry (IHC), immunofluorescence (IF), double-IF (d-IF), histochemistry, quantitative reverse transcription PCR (qPCR) and *in situ* hybridization (ISH). We defined four different stromal compartments in surgical specimens of PC: the juxtatumoural, peripheral, lobular and septal stroma. Tissue microarrays were produced that contained all of the pre-defined compartments. Using a semi-quantitative 4-tiered scoring system, we evaluated the expression of 37 FB markers and 8 ECM markers to evaluate the compartment-specific expression of each individual marker.

Research results
In this study, we found that CD10, CD271, cytoglobin, DOG1, miR-21, nestin, and tenascin C exhibited significant differences in expression profiles between the juxtatumoural and peripheral compartments of the PC stroma. CD10, cytoglobin, DOG1, miR-21, and nestin were all expressed at significantly higher levels in j-CAFs than in p-CAFs. Similarly, tenascin C was more abundantly expressed in juxtatumoural ECM than in peripheral ECM. CD271 was the only of the examined markers to be expressed at higher levels in p-CAFs than in j-CAFs. A combination of the markers cytoglobin, CD271, and miR-21 can be used to identify the different immune phenotypic subpopulations of CAFs in PC.

Research conclusions
In the present study, by using d-IF for multiple combinations of markers as well as conventional IHC, IF, and *ISH*, we were able to identify different immune phenotypic subpopulations of CAFs in the PC stroma. Using a panel of immunohistochemical biomarkers, we could distinguish two immunophenotypically different populations of CAFs: Juxtatumoural CAFs (j-CAFs), which were in very close vicinity to the cancer cells, and peripheral CAFs (p-CAFs), which were located > 100 μm away from the cancer cells. Interestingly, some of the markers that we identified to be predominantly expressed in j-CAFs (CD10, miR-21) have previously been demonstrated to have negative prognostic value in PC, whereas CD271, a marker that we found to be expressed mainly in p-CAFs, has been shown to hold positive prognostic value in PC. These findings may indicate that j-CAFs may be involved in an "unholy alliance" with the cancer cells, whereas p-CAFs may promote reduction of tumour growth. Hence, CAF heterogeneity in PC may explain some of the previously published, seemingly conflicting data regarding the role of CAFs in PC progression. The findings from this study could indicate that the composition of CAF subtypes in the desmoplastic stroma of PC could affect the outcomes

of individual patients. Furthermore, in the future, the stromal CAF composition may possibly be used as a marker to evaluate whether a specific PC patient might benefit from stroma-modulating therapies.

Research perspectives

This study indicates that it is too simplistic to view the CAF population in PC as a homogeneous cell population. Instead, at least two immune phenotypic subpopulations of CAFs can be characterized by different biomarker profiles. Future studies should determine whether the different CAF subpopulations in PC hold prognostic value or have different functional properties. Furthermore, CAF heterogeneity could provide an opportunity for the development of therapies aiming at the modulation of only one CAF subpopulation instead of targeting the entire CAF population in PC.

ACKNOWLEDGMENTS

REFERENCES

1   **Siegel RL**, Miller KD, Jemal A. Cancer statistics, 2018. *CA Cancer J Clin* 2018; **68**: 7-30 [PMID: 29313949 DOI: 10.3322/caac.21442]

2   **Ansari D**, Tingstedt B, Andersson B, Holmquist F, Sturesson C, Williamsson C, Sasor A, Borg D, Bauden M, Andersson R. Pancreatic cancer: yesterday, today and tomorrow. *Future Oncol* 2016; **12**: 1929-1946 [PMID: 27246628 DOI: 10.2217/fon-2016-0010]

3   **Erkan M**, Hausmann S, Michalski CW, Schlitter AM, Fingerle AA, Dobritz M, Friess H, Kleeff J. How fibrosis influences imaging and surgical decisions in pancreatic cancer. *Front Physiol* 2012; **3**: 389 [PMID: 23060813 DOI: 10.3389/fphys.2012.00389]

4   **Kadaba R**, Birke H, Wang J, Hooper S, Andl CD, Di Maggio F, Soylu E, Ghallab M, Bor D, Froeling FE, Bhattacharya S, Rustgi AK, Sahai E, Chelala C, Sasieni P, Kocher HM. Imbalance of desmoplastic stromal cell numbers drives aggressive cancer processes. *J Pathol* 2013; **230**: 107-117 [PMID: 23359139 DOI: 10.1002/path.4172]

5   **Heldin CH**, Rubin K, Pietras K, Ostman A. High interstitial fluid pressure - an obstacle in cancer therapy. *Nat Rev Cancer* 2004; **4**: 806-813 [PMID: 15510161 DOI: 10.1038/nrc1456]

6   **Provenzano PP**, Cuevas C, Chang AE, Goel VK, Von Hoff DD, Hingorani SR. Enzymatic targeting of the stroma ablates physical barriers to treatment of pancreatic ductal adenocarcinoma. *Cancer Cell* 2012; **21**: 418-429 [PMID: 22439937 DOI: 10.1016/j.ccr.2012.01.007]

7   **Erkan M**, Kleeff J, Gorbachevski A, Reiser C, Mitkus T, Esposito I, Giese T, Büchler MW, Giese NA, Friess H. Periostin creates a tumor-supportive microenvironment in the pancreas by sustaining fibrogenic stellate cell activity. *Gastroenterology* 2007; **132**: 1447-1464 [PMID: 17408641 DOI: 10.1053/j.gastro.2007.01.031]

8   **Erkan M**, Adler G, Apte MV, Bachem MG, Buchholz M, Detlefsen S, Esposito I, Friess H, Gress TM, Habisch HJ, Hwang RF, Jaster R, Kleeff J, Klöppel G, Kordes C, Logsdon CD, Masamune A, Michalski CW, Oh J, Phillips PA, Pinzani M, Reiser-Erkan C, Tsukamoto H, Wilson J. StellaTUM: current consensus and discussion on pancreatic stellate cell research. *Gut* 2012; **61**: 172-178 [PMID: 22115911 DOI: 10.1136/gutjnl-2011-301220]

9   **Apte MV**, Haber PS, Applegate TL, Norton ID, McCaughan GW, Korsten MA, Pirola RC, Wilson JS. Periacinar stellate shaped cells in rat pancreas: identification, isolation, and culture. *Gut* 1998; **43**: 128-133 [PMID: 9771417 DOI: 10.1136/gut.43.1.128]

10   **Apte MV**, Wilson JS, Lugea A, Pandol SJ. A starring role for stellate cells in the pancreatic cancer microenvironment. *Gastroenterology* 2013; **144**: 1210-1219 [PMID: 23622130 DOI: 10.1053/j.gastro.2012.11.037]

11   **Vonlaufen A**, Phillips PA, Xu Z, Goldstein D, Pirola RC, Wilson JS, Apte MV. Pancreatic stellate cells and pancreatic cancer cells: an unholy alliance. *Cancer Res* 2008; **68**: 7707-7710 [PMID: 18829522 DOI: 10.1158/0008-5472.CAN-08-1132]

12   **Heneberg P**. Paracrine tumor signaling induces transdifferentiation of surrounding fibroblasts. *Crit Rev Oncol Hematol* 2016; **97**: 303-311 [PMID: 26467073 DOI: 10.1016/j.critrevonc.2015.09.008]

13   **Hwang RF**, Moore T, Arumugam T, Ramachandran V, Amos KD, Rivera A, Ji B, Evans DB, Logsdon CD. Cancer-associated stromal fibroblasts promote pancreatic tumor progression. *Cancer Res* 2008; **68**: 918-926 [PMID: 18245495 DOI: 10.1158/0008-5472.CAN-07-5714]

14   **Vonlaufen A**, Joshi S, Qu C, Phillips PA, Xu Z, Parker NR, Toi CS, Pirola RC, Wilson JS, Goldstein D, Apte MV. Pancreatic stellate cells: partners in crime with pancreatic cancer cells. *Cancer Res* 2008; **68**: 2085-2093 [PMID: 18381413 DOI: 10.1158/0008-5472.CAN-07-2477]

15   **Pan B**, Liao Q, Niu Z, Zhou L, Zhao Y. Cancer-associated fibroblasts in pancreatic adenocarcinoma. *Future Oncol* 2015; **11**: 2603-2610 [PMID: 26284509 DOI: 10.2217/FON.15.176]

16   **Bachem MG**, Schünemann M, Ramadani M, Siech M, Beger H, Buck A, Zhou S, Schmid-Kotsas A, Adler G. Pancreatic carcinoma cells induce fibrosis by stimulating proliferation and matrix synthesis of stellate cells. *Gastroenterology* 2005; **128**: 907-921 [PMID: 15825074 DOI: 10.1053/j.gastro.2004.12.036]

17   **Sinn M**, Denkert C, Striefler JK, Pelzer U, Stieler JM, Bahra M, Lohneis P, Dörken B, Oettle H, Riess H, Sinn BV. α-Smooth muscle actin expression and desmoplastic stromal reaction in pancreatic cancer: results from the CONKO-001 study. *Br J Cancer* 2014; **111**: 1917-1923 [PMID: 25314063 DOI: 10.1038/bjc.2014.495]

18   **Erkan M**, Michalski CW, Rieder S, Reiser-Erkan C, Abiatari I, Kolb A, Giese NA, Esposito I, Friess H, Kleeff J. The activated stroma index is a novel and independent prognostic marker in pancreatic ductal adenocarcinoma. *Clin Gastroenterol Hepatol* 2008; **6**: 1155-1161 [PMID: 18639493 DOI: 10.1016/j.cgh.2008.05.006]

19   **Bachem MG**, Schneider E, Gross H, Weidenbach H, Schmid RM, Menke A, Siech M, Beger H, Grünert A, Adler G. Identification, culture, and characterization of pancreatic stellate cells in rats and humans. *Gastroenterology* 1998; **115**: 421-432 [PMID: 9679048 DOI: 10.1016/S0016-5085(98)70209-4]

20   **Mantoni TS**, Lunardi S, Al-Assar O, Masamune A, Brunner TB. Pancreatic stellate cells radioprotect pancreatic cancer cells through β1-integrin signaling. *Cancer Res* 2011; **71**: 3453-3458 [PMID: 21558392 DOI: 10.1158/0008-5472.CAN-10-1633]

21   **Hessmann E**, Patzak MS, Klein L, Chen N, Kari V, Ramu I, Bapiro TE, Frese KK, Gopinathan A, Richards FM, Jodrell DI, Verbeke C, Li X, Heuchel R, Löhr JM, Johnsen SA, Gress TM, Ellenrieder V, Neesse A. Fibroblast drug scavenging increases intratumoural gemcitabine accumulation in murine pancreas cancer. *Gut* 2018; **67**: 497-507 [PMID: 28077438 DOI: 10.1136/gutjnl-2016-311954]

22   **Ogier C**, Colombo PE, Bousquet C, Canterel-Thouennon L, Sicard P, Garambois V, Thomas G, Gaborit N, Jarlier M, Pirot N, Pugnière M, Vie N, Gongora C, Martineau P, Robert B, Pèlegrin A, Chardès T, Larbouret C. Targeting the NRG1/HER3 pathway in tumor cells and cancer-associated fibroblasts with an anti-neuregulin 1 antibody inhibits tumor growth in pre-clinical models of pancreatic cancer. *Cancer Lett* 2018; **432**: 227-236 [PMID: 29935372 DOI: 10.1016/j.canlet.2018.06.023]

23   **Feng R**, Morine Y, Ikemoto T, Imura S, Iwahashi S, Saito Y, Shimada M. Nab-paclitaxel interrupts cancer-stromal interaction through C-X-C motif chemokine 10-mediated interleukin-6 downregulation in vitro. *Cancer Sci* 2018; **109**: 2509-2519 [PMID: 29902349 DOI: 10.1111/cas.13694]

24   **Rhim AD**, Oberstein PE, Thomas DH, Mirek ET, Palermo CF, Sastra SA, Dekleva EN, Saunders T, Becerra CP, Tattersall IW, Westphalen CB, Kitajewski J, Fernandez-Barrena MG, Fernandez-Zapico ME, Iacobuzio-Donahue C, Olive KP, Stanger BZ. Stromal elements act to restrain, rather than support, pancreatic ductal adenocarcinoma. *Cancer Cell* 2014; **25**: 735-747 [PMID: 24856585 DOI: 10.1016/j.ccr.2014.04.021]

25   **Özdemir BC**, Pentcheva-Hoang T, Carstens JL, Zheng X, Wu CC, Simpson TR, Laklai H, Sugimoto H, Kahlert C, Novitskiy SV, De

Jesus-Acosta A, Sharma P, Heidari P, Mahmood U, Chin L, Moses HL, Weaver VM, Maitra A, Allison JP, LeBleu VS, Kalluri R. Depletion of carcinoma-associated fibroblasts and fibrosis induces immunosuppression and accelerates pancreas cancer with reduced survival. *Cancer Cell* 2014; **25**: 719-734 [PMID: 24856586 DOI: 10.1016/j.ccr.2014.04.005]

26   **Iacobuzio-Donahue CA**, Ryu B, Hruban RH, Kern SE. Exploring the host desmoplastic response to pancreatic carcinoma: gene expression of stromal and neoplastic cells at the site of primary invasion. *Am J Pathol* 2002; **160**: 91-99 [PMID: 11786403 DOI: 10.1016/S0002-9440(10)64353-2]

27   **Öhlund D**, Handly-Santana A, Biffi G, Elyada E, Almeida AS, Ponz-Sarvise M, Corbo V, Oni TE, Hearn SA, Lee EJ, Chio II, Hwang CI, Tiriac H, Baker LA, Engle DD, Feig C, Kultti A, Egeblad M, Fearon DT, Crawford JM, Clevers H, Park Y, Tuveson DA. Distinct populations of inflammatory fibroblasts and myofibroblasts in pancreatic cancer. *J Exp Med* 2017; **214**: 579-596 [PMID: 28232471 DOI: 10.1084/jem.20162024]

28   **Sugimoto H**, Mundel TM, Kieran MW, Kalluri R. Identification of fibroblast heterogeneity in the tumor microenvironment. *Cancer Biol Ther* 2006; **5**: 1640-1646 [PMID: 17106243 DOI: 10.4161/cbt.5.12.3354]

29   **Haeberle L**, Steiger K, Schlitter AM, Safi SA, Knoefel WT, Erkan M, Esposito I. Stromal heterogeneity in pancreatic cancer and chronic pancreatitis. *Pancreatology*; Epub ahead of print: May 12, 2018 [PMID: 29778400 DOI: 10.1016/j.pan.2018.05.004]

30   **Ene-Obong A**, Clear AJ, Watt J, Wang J, Fatah R, Riches JC, Marshall JF, Chin-Aleong J, Chelala C, Gribben JG, Ramsay AG, Kocher HM. Activated pancreatic stellate cells sequester CD8+ T cells to reduce their infiltration of the juxtatumoral compartment of pancreatic ductal adenocarcinoma. *Gastroenterology* 2013; **145**: 1121-1132 [PMID: 23891972 DOI: 10.1053/j.gastro.2013.07.025]

31   **Rubie C**, Kempf K, Hans J, Su T, Tilton B, Georg T, Brittner B, Ludwig B, Schilling M. Housekeeping gene variability in normal and cancerous colorectal, pancreatic, esophageal, gastric and hepatic tissues. *Mol Cell Probes* 2005; **19**: 101-109 [PMID: 15680211 DOI: 10.1016/j.mcp.2004.10.001]

32   **Hellemans J**, Mortier G, De Paepe A, Speleman F, Vandesompele J. qBase relative quantification framework and software for management and automated analysis of real-time quantitative PCR data. *Genome Biol* 2007; **8**: R19 [PMID: 17291332 DOI: 10.1186/gb-2007-8-2-r19]

33   **Nielsen BS**, Jørgensen S, Fog JU, Søkilde R, Christensen IJ, Hansen U, Brünner N, Baker A, Møller S, Nielsen HJ. High levels of microRNA-21 in the stroma of colorectal cancers predict short disease-free survival in stage II colon cancer patients. *Clin Exp Metastasis* 2011; **28**: 27-38 [PMID: 21069438 DOI: 10.1007/s10585-010-9355-7]

34   **Anderson CM**, Zhang B, Miller M, Butko E, Wu X, Laver T, Kernag C, Kim J, Luo Y, Lamparski H, Park E, Su N, Ma XJ. Fully Automated RNAscope In Situ Hybridization Assays for Formalin-Fixed Paraffin-Embedded Cells and Tissues. *J Cell Biochem* 2016; **117**: 2201-2208 [PMID: 27191821 DOI: 10.1002/jcb.25606]

35   **Nakatani K**, Okuyama H, Shimahara Y, Saeki S, Kim DH, Nakajima Y, Seki S, Kawada N, Yoshizato K. Cytoglobin/STAP, its unique localization in splanchnic fibroblast-like cells and function in organ fibrogenesis. *Lab Invest* 2004; **84**: 91-101 [PMID: 14647402 DOI: 10.1038/sj.labinvest.3700013]

36   **Spector I**, Honig H, Kawada N, Nagler A, Genin O, Pines M. Inhibition of pancreatic stellate cell activation by halofuginone prevents pancreatic xenograft tumor development. *Pancreas* 2010; **39**: 1008-1015 [PMID: 20442678 DOI: 10.1097/MPA.0b013e3181da8aa3]

37   **Nielsen MFB**, Mortensen MB, Detlefsen S. Identification of markers for quiescent pancreatic stellate cells in the normal human pancreas. *Histochem Cell Biol* 2017; **148**: 359-380 [PMID: 28540429 DOI: 10.1007/s00418-017-1581-5]

38   **Zion O**, Genin O, Kawada N, Yoshizato K, Roffe S, Nagler A, Iovanna JL, Halevy O, Pines M. Inhibition of transforming growth factor beta signaling by halofuginone as a modality for pancreas fibrosis prevention. *Pancreas* 2009; **38**: 427-435 [PMID: 19188864

DOI: 10.1097/MPA.0b013e3181967670]

39   **Matsuda Y**, Hagio M, Ishiwata T. Nestin: a novel angiogenesis marker and possible target for tumor angiogenesis. *World J Gastroenterol* 2013; **19**: 42-48 [PMID: 23326161 DOI: 10.3748/wjg.v19.i1.42]

40   **Yamahatsu K**, Matsuda Y, Ishiwata T, Uchida E, Naito Z. Nestin as a novel therapeutic target for pancreatic cancer via tumor angiogenesis. *Int J Oncol* 2012; **40**: 1345-1357 [PMID: 22246533 DOI: 10.3892/ijo.2012.1333]

41   **Ikenaga N**, Ohuchida K, Mizumoto K, Cui L, Kayashima T, Morimatsu K, Moriyama T, Nakata K, Fujita H, Tanaka M. CD10+ pancreatic stellate cells enhance the progression of pancreatic cancer. *Gastroenterology* 2010; **139**: 1041-1051, 1051.e1-1051.e8 [PMID: 20685603 DOI: 10.1053/j.gastro.2010.05.084]

42   **Fujiwara K**, Ohuchida K, Mizumoto K, Shindo K, Eguchi D, Kozono S, Ikenaga N, Ohtsuka T, Takahata S, Aishima S, Tanaka M. CD271+ subpopulation of pancreatic stellate cells correlates with prognosis of pancreatic cancer and is regulated by interaction with cancer cells. *PLoS One* 2012; **7**: e52682 [PMID: 23300742 DOI: 10.1371/journal.pone.0052682]

43   **Dang C**, Zhang Y, Ma Q, Shimahara Y. Expression of nerve growth factor receptors is correlated with progression and prognosis of human pancreatic cancer. *J Gastroenterol Hepatol* 2006; **21**: 850-858 [PMID: 16704535 DOI: 10.1111/j.1440-1746.2006.04074.x]

44   **Hemminger J**, Marsh WL, Iwenofu OH, Frankel WL. DOG1 (clone K9) is seldom expressed and not useful in the evaluation of pancreatic neoplasms. *Appl Immunohistochem Mol Morphol* 2012; **20**: 397-401 [PMID: 22495382 DOI: 10.1097/PAI.0b013e318246c345]

45   **Zhang L**, Yao J, Li W, Zhang C. Micro-RNA-21 Regulates Cancer-Associated Fibroblast-Mediated Frug Resistance in Pancreatic Cancer. *Oncol Res* 2017 [PMID: 28477403 DOI: 10.3727/096504017X14934840662335]

46   **Rask L**, Balslev E, Jørgensen S, Eriksen J, Flyger H, Møller S, Høgdall E, Litman T, Nielsen BS. High expression of miR-21 in tumor stroma correlates with increased cancer cell proliferation in human breast cancer. *APMIS* 2011; **119**: 663-673 [PMID: 21917003 DOI: 10.1111/j.1600-0463.2011.02782.x]

47   **Giovannetti E**, Funel N, Peters GJ, Del Chiaro M, Erozenci LA, Vasile E, Leon LG, Pollina LE, Groen A, Falcone A, Danesi R, Campani D, Verheul HM, Boggi U. MicroRNA-21 in pancreatic cancer: correlation with clinical outcome and pharmacologic aspects underlying its role in the modulation of gemcitabine activity. *Cancer Res* 2010; **70**: 4528-4538 [PMID: 20460539 DOI: 10.1158/0008-5472.CAN-09-4467]

48   **Kadera BE**, Li L, Toste PA, Wu N, Adams C, Dawson DW, Donahue TR. MicroRNA-21 in pancreatic ductal adenocarcinoma tumor-associated fibroblasts promotes metastasis. *PLoS One* 2013; **8**: e71978 [PMID: 23991015 DOI: 10.1371/journal.pone.0071978]

49   **Ali S**, Suresh R, Banerjee S, Bao B, Xu Z, Wilson J, Philip PA, Apte M, Sarkar FH. Contribution of microRNAs in understanding the pancreatic tumor microenvironment involving cancer associated stellate and fibroblast cells. *Am J Cancer Res* 2015; **5**: 1251-1264 [PMID: 26046003]

50   **Juuti A**, Nordling S, Louhimo J, Lundin J, Haglund C. Tenascin C expression is upregulated in pancreatic cancer and correlates with differentiation. *J Clin Pathol* 2004; **57**: 1151-1155 [PMID: 15509674 DOI: 10.1136/jcp.2003.015818]

51   **Esposito I**, Penzel R, Chaib-Harrireche M, Barcena U, Bergmann F, Riedl S, Kayed H, Giese N, Kleeff J, Friess H, Schirmacher P. Tenascin C and annexin II expression in the process of pancreatic carcinogenesis. *J Pathol* 2006; **208**: 673-685 [PMID: 16450333 DOI: 10.1002/path.1935]

52   **Jones FS**, Jones PL. The tenascin family of ECM glycoproteins: structure, function, and regulation during embryonic development and tissue remodeling. *Dev Dyn* 2000; **218**: 235-259 [PMID: 10842355 DOI: 10.1002/(SICI)1097-0177(200006)218:2<235::AID-DVDY2>3.0.CO;2-G]

53   **Xu Y**, Li Z, Jiang P, Wu G, Chen K, Zhang X, Li X. The co-expression of MMP-9 and Tenascin-C is significantly associated with the progression and prognosis of pancreatic cancer. *Diagn Pathol* 2015; **10**: 211 [PMID: 26652622 DOI: 10.1186/s13000-015-0445-3]

54   **Paron I**, Berchtold S, Vörös J, Shamarla M, Erkan M, Höfler H, Esposito I. Tenascin-C enhances pancreatic cancer cell growth and motility and affects cell adhesion through activation of the integrin pathway. *PLoS One* 2011; **6**: e21684 [PMID: 21747918 DOI: 10.1371/journal.pone.0021684]

55   **Hayasaki A**, Murata Y, Usui M, Hibi T, Ito T, Iizawa Y, Kato H, Tanemura A, Azumi Y, Kuriyama N, Kishiwada M, Mizuno S, Sakurai H, Yoshida T, Isaji S. Clinical Significance of Histological Effect and Intratumor Stromal Expression of Tenascin-C in Resected Specimens After Chemoradiotherapy for Initially Locally Advanced Unresectable Pancreatic Ductal Adenocarcinoma. *Pancreas* 2018; **47**: 390-399 [PMID: 29517632 DOI: 10.1097/MPA.0000000000001022]

56   **Gore J**, Korc M. Pancreatic cancer stroma: friend or foe? *Cancer Cell* 2014; **25**: 711-712 [PMID: 24937454 DOI: 10.1016/j.ccr.2014.05.026]

57   **Olive KP**, Jacobetz MA, Davidson CJ, Gopinathan A, McIntyre D, Honess D, Madhu B, Goldgraben MA, Caldwell ME, Allard D, Frese KK, Denicola G, Feig C, Combs C, Winter SP, Ireland-Zecchini H, Reichelt S, Howat WJ, Chang A, Dhara M, Wang L, Rückert F, Grützmann R, Pilarsky C, Izeradjene K, Hingorani SR, Huang P, Davies SE, Plunkett W, Egorin M, Hruban RH, Whitebread N, McGovern K, Adams J, Iacobuzio-Donahue C, Griffiths J, Tuveson DA. Inhibition of Hedgehog signaling enhances delivery of chemotherapy in a mouse model of pancreatic cancer. *Science* 2009; **324**: 1457-1461 [PMID: 19460966 DOI: 10.1126/science.1171362]

58   **Nielsen MF**, Mortensen MB, Detlefsen S. Key players in pancreatic cancer-stroma interaction: Cancer-associated fibroblasts, endothelial and inflammatory cells. *World J Gastroenterol* 2016; **22**: 2678-2700 [PMID: 26973408 DOI: 10.3748/wjg.v22.i9.2678]

59   **Ko AH**, LoConte N, Tempero MA, Walker EJ, Kate Kelley R, Lewis S, Chang WC, Kantoff E, Vannier MW, Catenacci DV, Venook AP, Kindler HL. A Phase I Study of FOLFIRINOX Plus IPI-926, a Hedgehog Pathway Inhibitor, for Advanced Pancreatic Adenocarcinoma. *Pancreas* 2016; **45**: 370-375 [PMID: 26390428 DOI: 10.1097/MPA.0000000000000458]

60   **Sobin L,** Gospodarowicz M, Wittekind C. TNM Classification of Malignant Tumours. 7th ed. New York: International Union Against Cancer (UICC), 2009: 1-336

Baishideng®